Sheffield Hallam University

Influence of curing on pore properties and strength of alkali activated mortars

MANGAT, Pal <http://orcid.org/0000-0003-1736-8891> and OJEDOKUN, Olalekan <http://orcid.org/0000-0002-9573-4976>

Available from Sheffield Hallam University Research Archive (SHURA) at:

http://shura.shu.ac.uk/22442/

Published version

Sheffield Hallam University Research Archive
http://shura.shu.ac.uk

1 # Influence of curing on pore properties and strength of alkali
2 # activated mortars

3 P.S. Mangat and Olalekan O. Ojedokun

4 Centre for Infrastructure Management, Materials and Engineering Research Institute, Sheffield Hallam

5 University, Sheffield S1 1WB, UK

6 **ABSTRACT**

7 The paper investigates the effect of wet/dry, wet and dry curing on the pore properties and

8 strength of an alkali activated cementitious (AACM) mortar. The pore characteristics were

9 determined from the cumulative and differential pore volume curves obtained by mercury

10 intrusion porosimetry. AACM mortars possess a bimodal pore size distribution while the

11 control PC mortar is unimodal. AACM mortars have a lower porosity, higher capillary pore

12 volume, lower gel pore volume and lower critical and threshold pore diameters than the PC

13 mortar which indicate greater durability potential of AACMs. Wet/dry curing is optimum for

14 AACM mortars while wet curing is optimum for the PC mortar. Shrinkage and retarding

15 admixtures improve the strength and pore structure of the AACMs.

16

17

18

19

20

21

22

23

26

27

28

29

30

31

32

33

34

35

36

37

38

39

40

41

42 **Notations:**

43 AACM   Alkali activated cementitious materials

44 PC   Portland cement

45 GGBS   Ground granulated blast-furnace slag

46 ITZ   Interfacial transition zone

47 p Absolute applied pressure

48 r Pore radius

49 y Mercury surface tension (= 0.48N/m)

50 ϕ Mercury contact angle (= 140^{0})

2

1.0 Introduction

The use of alkali activated cementitious materials (AACM) in place of Portland cement (PC) has been recognized to have great potential in construction applications. There is the need for a viable alternative to PC because of the high carbon footprint generated during its production with a huge energy demand, which is not sustainable in the future. The carbon footprint is significant because of the large volume of Portland cement PC consumed worldwide, which is ranked second after the volume of water [1]. To put this into perspective, for each tonne of cement produced an equivalent tonne of CO_2 is emitted into the atmosphere. This translates to the emission of 400 Kg of CO_2 per 1 m^3 of concrete production [2]. In addition, the cement industry consumes between 12 - 15% of the total industrial energy use [3]. The electric energy consumption for the burning process during cement production is estimated to be 65 kWh/tonne while the thermal energy consumption for cement grinding is 2.72 GJ/tonne [3]. Clearly, there is a dire need for reducing this carbon foot print and energy demand.

Limited knowledge is available in literature on the pore properties of AACMs and geopolymers [4]. However, established knowledge on the pore properties of conventional concrete [5] shows their critical importance in controlling the durability and strength of concrete. The pore properties are equally important for AACMs and other porous ceramic materials. The refinement of concrete pore structure improves its compressive strength, resistance to diffusion of deleterious substances such as chlorides and CO_2, which affect its durability [6]. These deleterious substances which cause corrosion of steel in concrete are transported through the concrete pores by capillary absorption, hydrostatic pressure and diffusion [7]. Diffusion of the ionic elements (Cl^- and Na^+) is mainly through the pores of the cement paste matrix and not through the interface between cement paste and aggregates [8]. The interface between the cement paste and aggregates accounts for up to 50% of the total

3

75 volume of pores in hardened concrete but these were found to be discontinuous and isolated

76 from each other, thereby preventing the penetration of harmful elements through them [8].

77 The little understanding of the pore properties of AACM concrete provided in current

78 literature suggests that the pore size distribution of AACMs is bimodal under all curing

79 conditions [2,4]. The pores of AACMs are separated into two zones (> 1µm and < 0.02µm

80 ranges) unlike a similar grade of PC matrix which is observed to be unimodal ranging

81 between 0.01µm to 0.1µm [2,4]. Literature suggests that the gel pores in AACMs are formed

82 during the polymerization of aluminosilicate gel during curing [9]. The extent of gel pores

83 formed under different curing regimes is not understood. The gel pores are defined to be

84 within the range of 0.005 to 0.01 µm based on PC concrete research [9]. The large capillary

85 pores which are orders of magnitude bigger than gel pores and are within the range of 0.01

86 µm to 100 µm based on PC concrete research [9]. *Yue and Jiaqi* [10] showed an inverse

87 relationship between the volume of gel and capillary pores as hydration progresses in PC

88 concrete. During the hydration process of concrete, the volume of capillary pores decreases

89 while the gel pores increases. This results in a lower cumulative pore volume in time because

90 the comparatively large capillary pores is partially occupied by the binder gel. Ultimately, a

91 denser microstructure evolves as the hydration progresses. The influence of curing on the

92 pore properties of AACMs such as the gel pores, capillary pores, critical and threshold pore

93 diameters are not defined in literature. These aspects of pore properties of AACMs are

94 reported in this paper.

95 Pore refinement of PC concrete is achieved by high humidity (> 80% R.H) curing which

96 provides prolonged hydration of cement at low or high temperatures [5]. In the case of

97 AACMs, earlier research has shown a need for high temperature curing at 50 - 80^{0}C, such as

98 steam or dry heat, for optimum geopolymerization reaction [2,11]. More recent work uses

99 ambient temperature (20 ± 2^{0}C), which is practical on construction site, for curing AACMs

100   [12,13]. The optimum levels of relative humidity required for AACM curing are not

101   established. However, results indicate that "dry" curing at low relative humidity (e.g. 60%

102   R.H.) produces high strength for AACMs unlike PC concrete which has maximum strength

103   under wet curing (100% R.H.) [14,15]. This can be beneficial for practical use of AACMs

104   since insitu curing in construction does not provide idealized wet conditions. Practical site

105   conditions represent a balance between, wet, wet/dry and dry conditions by preventing

106   moisture loss at early age while concrete is exposed to ambient conditions of wetting and

107   drying in the longer term. The practical curing conditions wet/dry, dry and wet at ambient

108   temperature applicable in the field, were adopted in this investigation to determine the

109   benefits of early age moisture available for curing on the strength and pore properties of

110   AACMs.

111   A potassium-based activator used in AACMs reduces the mean pore diameter more than a

112   sodium-based activator [4] while the total porosity of an alkali activated blast furnace slag

113   (BFS) is reduced by the inclusion of a high modulus (more concentrated) activator and low

114   water content in the mix [2]. The influence of chemical admixtures such as retarder and

115   shrinkage reducing admixtures on the pore properties of AACMs is not known. This aspect

116   together with the influence of activator dilution on the pore properties of AACM mortar is

117   investigated.

118   Mercury intrusion porosimetry (MIP) is the common test method for investigating the

119   microstructure of concrete. This is performed by applying mercury under high pressure

120   through concrete pores. The method is based on the "non-wetting" property of mercury on the

121   walls of the concrete pores. Mercury intrusion into the concrete matrix is suitable for pores

122   within the range of 0.003 to 400 μm [16]. This method is used for analysing the accessible

123   pores within the AACM and the control PC mortar samples in this investigation.

124 This paper is part of a comprehensive durability investigation of AACMs (mortar and

125 concrete) being undertaken by the authors. It characterises the basic pore-properties of the

126 material to provide a deeper understanding of the durability properties of reinforced AACM

127 concrete.

128 **2.0   Experimental programme**

129 *2.1   Materials and mixes*

130 The control PC mortar had a composition of 1: 2.1 (by weight) of CEM 1 cement to CEN

131 standard sand with a water/cement ratio of 0.47. The CEM 1 cement used is 42.5 Portland

132 cement and it was supplied by Frank Key group, Sheffield, UK. The PC mortar was produced

133 in accordance with BS EN 196-1:2016 [17]. The corresponding AACM 1 and 2 mortar mixes

134 comprised of GGBS binder, sodium silicate and hydroxide based activator, fine aggregate of

135 80% particle size passing 1mm sieve, liquid/binder ratio of 0.47 (alkali activator + water), a

136 shrinkage reducing admixture SRA and retarder R42. The fresh AACM 1 and 2 mortar mixes

137 were designed to achieve a flow of about 15 cm using the flow table test method [18]. The

138 shrinkage reducing admixture SRA was added to reduce the shrinkage of AACMs while

139 retarder R42 was added to increase the setting time. AACM 1 and 2 mixes were investigated

140 to provide optimum properties of the fresh and hardened material for practical applications.

141 However, AACM 1a and 2a mixes were also prepared with the same mix proportions but

142 without admixtures to provide data for direct comparison with the PC mix which also did not

143 contain admixtures. The mix compositions for AACM 1, 2, 1a, 2a and the control PC mortars

144 are presented in Table 1. Table 2 shows the chemical composition of Portland cement (PC)

145 and ground granulated blast-furnace slag (GGBS) binders used in the tests.

146 The average 28-day strength of the AACM and control PC mixes were designed to be fairly

147 similar under wet curing, based on trial mixes. Wet curing is the standard method for quality

148 testing of concrete [5]. The different curing methods adopted in this research are detailed in

149 section 2.2.

150 Table 1: Composition of the AACM and control PC mortars

Mix	Binder (%)	Fine Agg. (%)	Liquid (%)	Liquid/Binder Ratio	Activator Dilution (%)	R42 (% binder)	SRA (% binder)
AACM 1	49	28.0	23.0	0.47	0	0.75	2.0
AACM 2	49	28.0	23.0	0.47	7.76	0.75	2.0
AACM 1a	49	28.0	23.0	0.47	0	-	-
AACM 2a	49	28.0	23.0	0.47	7.76	-	-
Control PC	28	59.0	13.0	0.47	-	-	-

151 Table 2: Chemical composition of Portland cement and GGBS binders

Chemical component	SiO_2	Al_2O_3	Fe_2O_3	CaO	MgO	K_2O	Na_2O	TiO_2	P_2O_5	MnO	SO_3
PC (mass %)	11.1	8.35	3.16	64.2	2.09	1.19	0.227	1.88	2.01	2.14	3.64
GGBS (mass %)	28.6	12.4	5.7	42.3	6.1	0.8	0.4	1.78	<0.1	0.3	0.08

152 Sodium silicate activator of molarity 6.5 mol/L and modulus 2% was used for the AACM

153 mixes to provide optimum viscosity for controlling workability and setting time [19]. The

154 molarity of NaOH activator used was 4.8 mol/L. The combined molarity of the activators was

155 at the lower end of values used by other researchers [20] for a similar activator combination.

156 The activator for AACM 2 mixes was diluted with water at 7.76% (Table 1). The retarder

157 R42 is made from a blend of high grade Polyhydroxycarboxylic acid derivatives while the

158 shrinkage reducing admixtures (SRA) is made from Alkyl-ether. Each admixture contained

159 less than 0.1% chloride ion and 3.5% sodium oxide.

160 *2.2   Casting and curing*

161 The GGBS binder and saturated surface dry fine aggregate were placed in a 12 litre, 3 speed

162 Hobart mixer. They were mixed for 30 seconds at the lowest speed (option-1) to avoid

163 dispersing the powder into the atmosphere. The liquid component containing the activator

164 and retarder R42 were slowly added to the mix. Mixing continued for 2 minutes until a

165 uniform texture was produced. The shrinkage reducing admixture SRA was then slowly

166 added while mixing continued. The mortar was further mixed for 1 minute before stopping.

167 The control PC mortar and the AACM mixes without admixtures were prepared in a similar

168 manner without adding retarder R42 and shrinkage reducing admixture SRA. The AACM

169 and control PC mortars were cast in 75 x 75 x 75 mm steel cube moulds which had been

170 lightly oiled to prevent the hardened mortar from sticking to the surface. Three mortar cubes

171 were cast for each mix. The specimens were left covered in the moulds with polythene sheets

172 for 24 hours at room temperature of $20 \pm 2\ ^{0}C$ and a relative humidity of about 65%. The

173 specimens were demoulded 24 hrs after casting and were exposed to three different curing

174 regimes.

175 Three practical curing regimes (wet/dry, wet and dry), commonly applied in the construction

176 field, were adopted in this research work as shown in Table 3. Wet/dry curing involved

177 placing the mortar cubes in water at a temperature of $20 \pm 2^{0}C$ for 3 days immediately after

178 demoulding (24 hrs after casting), followed by dry curing in the laboratory air at a

179 temperature of $20 \pm 2^{0}C$ and approximately 65% relative humidity for 24 days (total curing

180 period of 28 days). Wet curing was provided by placing the cube specimens in water at a

181 temperature of $20 \pm 2\ ^{0}C$ for 27 days immediately after demoulding. Dry curing of the

182 mortars was provided by exposing them in the laboratory air at a temperature of $20 \pm 2^{0}C$ and

183 approximately 65% relative humidity for 27 days after demoulding. When cured in the

184 laboratory air (during wet/dry and dry curing), the specimens were securely covered with

185 polyethene sheets to prevent moisture loss from the concrete surface representing site practice

186 where different methods can be used to prevent rapid drying of concrete such as applying

187 curing membranes or covering concrete surface with wet hessian.

188   Table 3: Curing methods used for the AACM and control PC mortars

Samples	Age(days)	Wet/dry	Wet	Dry

		(Curing Medium)	(Curing Medium)	(Curing Medium)
75 mm cubes	0-3	Water	Water	Air
	3-28	Air	Water	Air
MIP samples	28-31	Oven (50^{0}C)	Oven (50^{0}C)	Oven (50^{0}C)
	31-34	Desiccator	Desiccator	Desiccator

189 *2.3   Test procedure*

190 *2.3.1   Compressive strength*

191 The compressive strength and density of the 75 mm mortar cubes were determined after 28

192 days curing under wet/dry, wet and dry regimes (Table 3). The compressive strength tests on

193 the cubes were conducted in accordance with *BS EN 12390-3:2009* [21]. The density of the

194 cubes was determined according to *BS EN 12390-7:2009* [22]. Three specimens were used to

195 determine the density and compressive strength of the 75 mm cubes. A loading rate of 3

196 MPa/min was applied during the compression testing and a post peak of 30% failure load was

197 programmed into the compression machine to prevent complete disintegration of the crushed

198 specimen. Samples for the Mercury intrusion porosimetry (MIP) tests were obtained from

199 these crushed samples.

200 *2.3.2   Mercury Intrusion Porosimetry*

201 Mercury intrusion porosimetry (MIP) test samples, with a weight of 1 - 2 g and average

202 length of 1 cm, were obtained from the crushed 75 mm mortar cubes. Errors caused by

203 hysteresis and entrapment of moisture during MIP testing was minimised by controlling the

204 dimensions, mass and drying of all test samples [23] as described here. The mercury intrusion

205 porosimetry (MIP) test samples were dried in an oven at a temperature of 50^{0}C for 3 days

206 (28- 31 days age) as shown in Table 3. Oven drying at a higher temperature than 50^{0}C causes

207 microcracking which may adversely affect the test results [24]. After oven drying for 3 days,

9

208   the samples were placed in a desiccator for another 3 days to reduce their temperature to

209   about 20^0C. The desiccator had silica gel at the bottom to further assist with removing

210   absorbed water and preventing moisture migration from the air. The drying and cooling were

211   carried out to remove absorbed water within the mortar pore system, which can obstruct its

212   accessible porosity during MIP testing.

213   MIP testing was performed using a Pascal 140/240 Porosimeter which is in two parts. Pascal

214   140 applies pressure of up to 100 MPa and Pascal 240 applies pressure of up to 200 MPa to

215   aid the intrusion of mercury through pore sizes down to 0.007 μm. The Pascal 140/240

216   Porosimeter measures pore sizes within the range of 0.007 to 100 μm. Its computer

217   microprocessor translates the data collected on the applied pressures to pore radius using the

218   Washburn equation (equation 1).

$$p = \frac{2y \cos \phi}{r} \qquad\qquad 1$$

219   Where p is the absolute applied pressure; r is the pore radius; y is the mercury surface

220   tension (= 0.48N/m); ϕ is the contact angle (= 140^0).

221   The limitation of Washburn equation is the assumption that the pores in the concrete matrix

222   are cylindrical in shape which has been criticised by researchers [23]. The graphs of pore

223   sizes and pore distribution were obtained at the end of the mercury intrusion porosimetry

224   analysis. The MIP analysis was performed on three test samples for each curing condition for
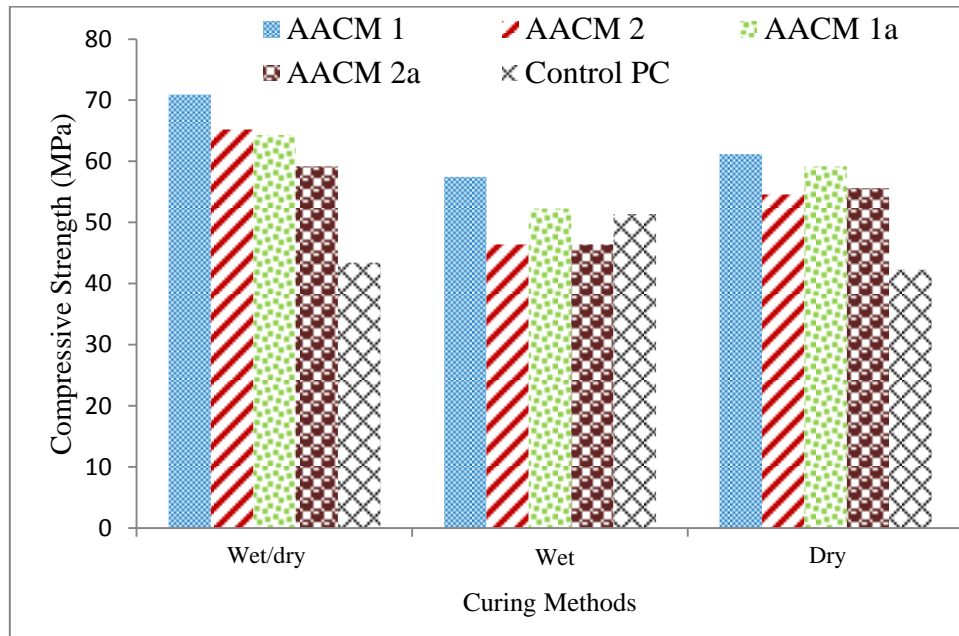
225   the AACM and control PC mortars.

226   **3.0**   **Results and discussion**

227   *3.1*   *Compressive strength and density*

228   The average value of the compressive strength and density of the three specimens tested per

229   mix had less than 5% variation.

230   *3.1.1*   *Effect of curing regimes on density and compressive strength*

231   The densities of the 75 mm mortar cubes at 28 days age are between 2.22 - 2.35 g/cm^3 for

232   wet/dry curing, 2.10 - 2.23 g/cm^3 for dry curing and 2.07 - 2.15 g/cm^3 for wet curing. The

233   corresponding 28day compressive strength for the AACM and control PC mortars under

234   wet/dry, wet and dry curing (Table 3) are shown in Fig. 1.

236   Fig. 1: Compressive strength of AACM and control PC mortars under wet/dry, wet and

237   dry curing at 28 days

238   The compressive strengths of AACM 1 are 70.9 MPa for wet/dry curing, 57.9 MPa for wet

239   curing, and 61.2 MPa for dry curing. The corresponding values for AACM 2 are 65.2 MPa,

240   46.4 MPa and 54.6 MPa. Similar trend is observed in AACM 1a and 2a. The wet/dry curing

241   method achieved the highest strength for all the AACM mortars. This curing method

242   involved 3 days wet curing at 20 ± 2^0C followed by 24 days in the laboratory air (20 ± 2^0C,

243   65% R.H.). The dry curing method of AACM 1 and 2 mortars (27 days curing in laboratory

244   air at 20 ± 2^0C, 65% R.H.) gave lower strength than the wet/dry method while wet curing (27

245   days curing in water at 20 ± 2^0C) gave the least compressive strength. The wet/dry curing of

246   AACM mixes gave the highest strength due to the formation of more crystalline

247   geopolymerisation products [2,11].

11

248 The effect of curing methods on the control PC mortar contrasts the AACM mortars by

249 providing the maximum compressive strength under wet curing. The availability of moisture

250 in the PC mortar supported cement hydration which produced more strength. The geopolymer

251 reactions in AACMs do not rely on moisture to the same extent as the hydration reactions in

252 PC. The control PC mortar recorded the highest compressive strength of 51.4 MPa (Fig. 1)

253 under wet curing followed by 43.4 MPa under wet/dry curing, which is slightly higher than

254 42.3 MPa under dry curing as shown in Fig. 1. The results of the control PC mortar are

255 consistent with other research which shows a similar effect of curing conditions on the

256 strength of PC concrete [25,26]. The relative humidity in the PC capillary pores is maintained

257 above 80% when cured in water, which favours hydration reactions [5]. There is little loss of

258 strength when PC concrete is cured in a moist medium above 80% R.H.

259 The 28 day strengths of AACM 1, 2 (both with retarder and shrinkage reducing admixture)

260 and PC mortar (without the admixture) under wet curing are 57.4 MPa, 52.3MPa and

261 51.4MPa respectively. The compressive strengths under wet curing of AACM mortars 1a and

262 2a (both without admixture) average 46.4 MPa and 46.2MPa respectively compared with

263 51.4MPa for wet cured PC mortar. The average strength of the AACM mixes is similar to the

264 PC mortar (control) mix under wet curing whereas their strength is much higher under

265 partially dry curing conditions (wet/dry and dry) which are encountered on site.

266 *3.1.2 Effect of activator dilution on compressive strength*

267 Fig. 1 shows the effect of activator dilution on the compressive strength of the AACM

268 mortars under wet/dry, wet and dry curing. The compressive strength decreases with

269 increasing dilution of activator. For example, the compressive strengths of AACM 1 mortar

270 were 70.9 MPa, 57.9 MPa and 61.2 MPa compared with 65.2 MPa, 46.4 MPa and 54.6 MPa

271 for AACM 2 mortar (7.76% dilution) under wet/dry, wet and dry curing respectively (Fig. 1).

272   Activator concentration is an effective factor in the geopolymerisation process in AACM

273   concrete. A reduction in strength has been reported when the activator concentration is not

274   sufficient for the geopolymerisation reaction [11,27]. Similarly, high activator concentration

275   will delay the AACM formations due to excessive cations, thereby limiting their mobility and

276   potential to interact with the reactive pozzolanic species [27]. This reverse effect of strength

277   reduction with increasing concentration of the alkali activator was, however, not observed in

278   this study.

279   *3.2   Pore size distribution*

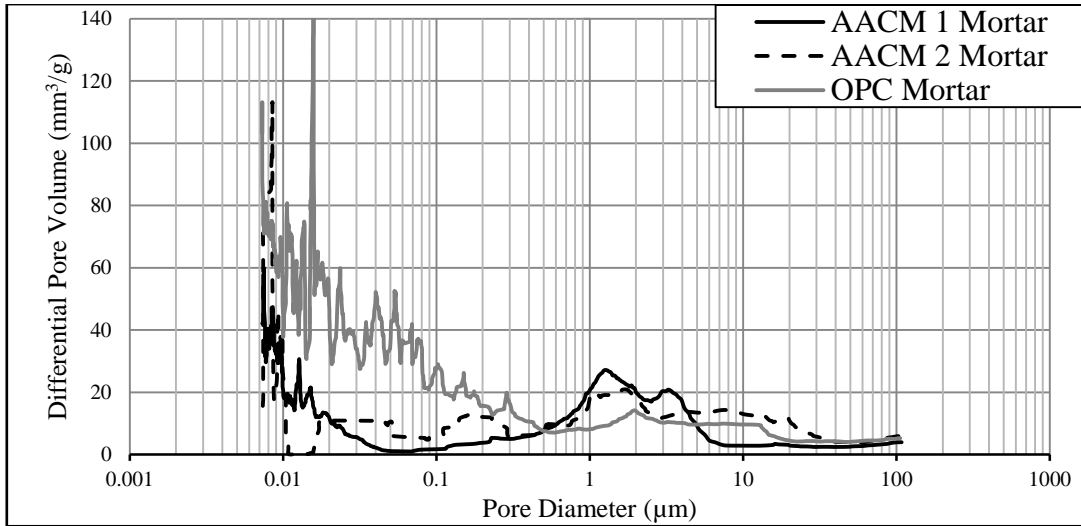280   *3.2.1   Unimodal and bimodal pore distribution*

281   The relationship between pore size and differential pore volume for AACM 1, 2 and the

282   control PC concrete under wet/dry, wet and dry curing are shown in Figures 2, 3 and 4
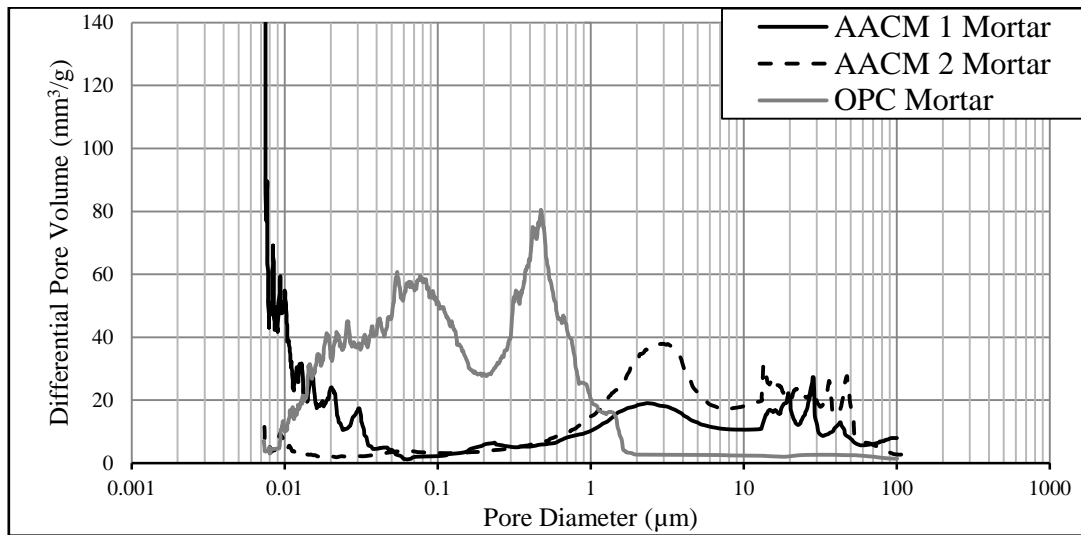
283   respectively.
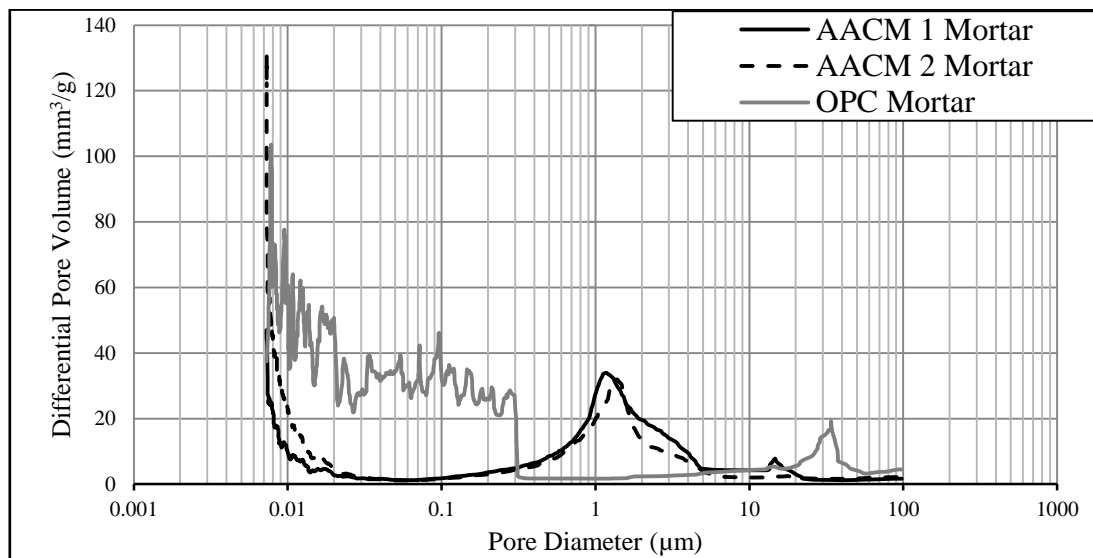
284

285   Fig. 2: Pore size distribution for AACM 1, 2 and control OPC mortars under wet/dry curing

13

286

Fig. 3: Pore size distribution for AACM 1, 2 and control OPC mortars under wet curing

287

288

Fig. 4: Pore size distribution for AACM 1, 2 and control OPC mortars under dry curing

289

290 The figures show the range of pore diameters under which significant levels of differential

291 pore volumes are observed and the range when the differential pore volume is at or near zero.

292 The diameter zones showing significant differential pore volume represent porosity whereas

293 the range indicating zero differential pore volume represents a non-porous zone. Based on

294 these criteria, it can be observed that the PC mortar has a unimodal pore distribution under

295 the three curing conditions shown in Figures 2, 3 and 4. The pore distribution is referred to as

296 unimodal when a single range of pore volume is observed within the differential pore volume

297 graphs [2,4]. The pore volume of the PC mortar falls within the range of 0.01 to 0.1 μm pore

14

298   diameter. Other studies on the microstructure of PC matrix also show a unimodal pore size

299   distribution with most of the pore volume within the range of 0.01 to 0.1 μm pore diameter

300   [2,4]. On the other hand, a double range of pore diameters with significant differential pore

301   volume which are separated by a diameter range with nearly zero differential pore volume is

302   categorized as a bimodal pore distribution [2,4]. These pore sizes are normally observed

303   between two separate zones of > 1 μm and <0.02 μm [2]. Figures 2, 3 and 4 show that

304   AACM 1 and 2 mortars fall under this category with significant porosity observed at > 1 μm

305   and <0.02 μm while there is little porosity between these pore size ranges.

306   The differences in the effects of wet/dry, wet and dry curing on the differential pore volumes

307   over the pore diameter ranges in Figures 2, 3 and 4 have been quantified by determining the

308   pore system parameters such as porosity and are discussed fully in section 3.3.

309   *Wet/dry curing*

310   The pore sizes in AACM 1 and 2 mortars subjected to wet/dry curing (Fig. 2) show a bimodal

311   pore size distribution. The first range of pore diameters showing significant differential pore

312   volumes in AACM 1 mortar is <0.02 μm while the second range is predominantly between

313   0.2 to 4.5 μm. There is insignificant differential pore volume between 0.02 and 0.2 μm

314   diameter. AACM 2 mortar shows a similar trend of bimodal pore distribution, the pore

315   diameters range from under 0.03 μm to greater than 0.2μm. On the other hand, the control PC

316   mortar shows a unimodal pore size distribution (Fig. 2) of diameter lesser than 0.3 μm. The

317   bimodal distribution of pores in AACM 1 and 2 mortars extends to larger pore diameters than

318   the control PC mortar; however the large pore size zone is isolated due to the bimodal

319   distribution, which will affect porosity as discussed in section 3.3.

320   *Wet curing*

321   The bimodal pore size distribution in AACM 2 mortar is less pronounced under wet curing

322   (Fig. 3) than under wet/dry (Fig. 2) or dry curing (Fig. 4). There is significant continuity of

15

323 pores between pore diameters 0.01 to 100 µm (particularly AACM 2) which is reflected by

324 the differential pore volume remaining slightly above zero in this pore diameter range. This

325 does not appear under both wet/dry and dry curing. Therefore some interconnection between

326 the gel pores (< 0.05 µm) and capillary pores (0.1 to 100 µm) is likely in wet cured AACM 2

327 mortar. The interconnection is represented by the regular distribution of peaks throughout the

328 range of pore sizes 0.01 to 100 µm (particularly AACM 2). The less solid gel products

329 produced in AACM 2 mortar due to the higher activator dilution may be insufficient to block

330 the interconnecting pores. Another reason for pore continuity could be the leaching of alkali

331 cations into the curing solution thereby resulting in loss of alkali concentration needed for

332 geopolymerisation reaction [28]. A slight degree of hydration reactions may also be a likely

333 contributor to the interconnection of pores under wet curing in the AACM 2 due to the high

334 degree of moist curing.

335 *Dry curing*

336 AACM 1 and 2 mortars under dry curing (Fig. 4) show a bimodal pore size distribution

337 similar to wet/dry curing. The first range of pores in AACM 1 mortar are less than 0.05 µm

338 while the second range of the bimodal pore size distribution is greater than 0.1 µm and

339 extends to 100 µm diameter. AACM 2 mortar has slightly different pore ranges of less than

340 0.02 µm and greater than 0.1 µm and extends to 100 µm diameter. The control PC mortar has

341 a unimodal pore distribution between 0.01 µm to approximately 2 µm, the pore diameter

342 range is higher than under wet/dry and wet curing. The PC mortar shows significant

343 differential pore volume within the dip between the two peaks in Figure 4, unlike the AACMs

344 where the differential pore volume reaches near zero between the bimodal peaks.

345 *3.3   Pore system parameters*

346 Pore system parameters are frequently used in analytical and empirical property-

347 microstructure relationship models [29,30]. These parameters are derived from the

16

348 cumulative porosity curves and logarithmic differential pore volume curves. They are

349 classified as intrudable porosity Φ_{in}, critical pore diameter d_c, threshold pore diameter d_{th} and

350 porosity [29,30]. The location of Φ_{in} is shown on the cumulative pore volume curve for both

351 PC and AACM mortars (Figures 5 and 6). The location of d_c and d_{th} is shown on the

352 corresponding differential pore volume curves in these figures. Two locations of d_c and d_{th}

353 are given on the bimodal graphs of AACM mortars. The porosity of cementitious material is

354 the percentage of pores in the total bulk volume of the mortar whereas intrudable porosity

355 represents only the pore volumes which are accesible to mecury intrusion [29]. The values of

356 these pore parameters are presented in Table 4. The porosity and pore volumes of AACM and

357 control PC mortars with and without shrinkage reducing admixture SRA and retarder R42 are

358 presented in Table 4.
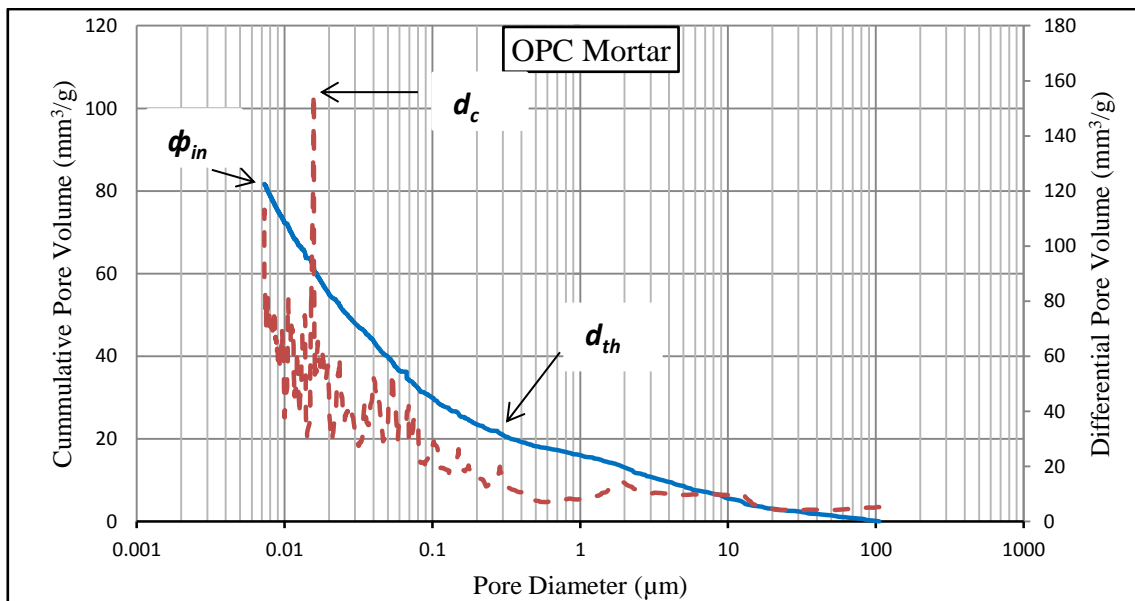
359

360 Fig. 5: Definition of Pore System Parameters in OPC Mortar (Authors' data)
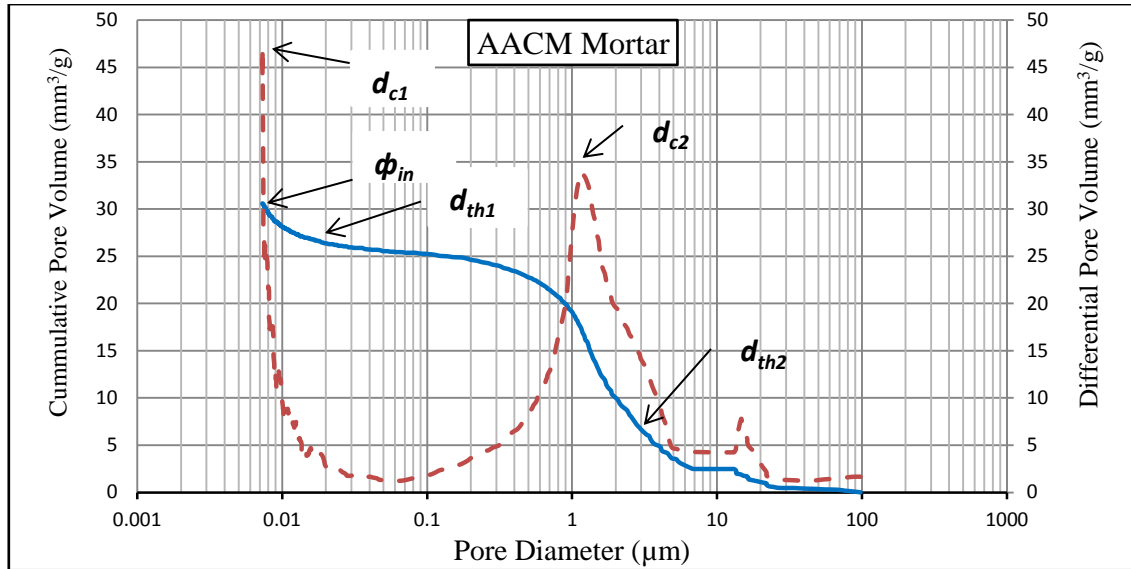
Fig. 6: Definition of Pore System Parameters in AACM Mortar (Authors' data)

Table 4: Pore system parameters for AACM and the control PC mortars

	Mix	Curing	Porosity		Pore diameters (µm)		Pore volumes (%)	
			Intrudable (mm³/g)	Porosity (%)	Critical d_{c1}	Threshold d_{th1}	Gel	Capillary
With admixtures	AACM 1	Wet/dry	29.68	4.64	0.0073	0.013	0.60	4.04
		wet	38.14	6.53	0.0073	0.014	0.66	5.87
		dry	53.44	9.90	0.0075	0.025	1.42	8.48
	AACM 2	Wet/dry	30.17	6.67	0.0073	0.021	0.98	5.69
		wet	45.48	8.02	0.0081	0.034	0.91	7.11
		dry	59.13	10.70	0.0085	0.048	1.65	9.05
Without admixtures	AACM 1a	Wet/dry	44.26	7.71	0.0081	0.018	0.26	7.45
		wet	51.66	9.05	0.0082	0.019	0.97	8.08
		dry	65.64	11.93	0.0084	0.032	1.92	10.01
	AACM 2a	Wet/dry	46.92	9.14	0.0086	0.027	1.18	7.96
		wet	53.83	10.13	0.0087	0.032	1.80	8.33
		dry	68.05	11.69	0.0089	0.051	1.96	9.73
	Control PC	Wet/dry	81.62	14.02	0.049	0.35	10.83	3.19
		wet	68.16	13.30	0.016	0.28	8.6	4.70
		dry	93.51	17.43	1.07	1.12	10.58	6.85

3.3.1 Intrudable pore volume

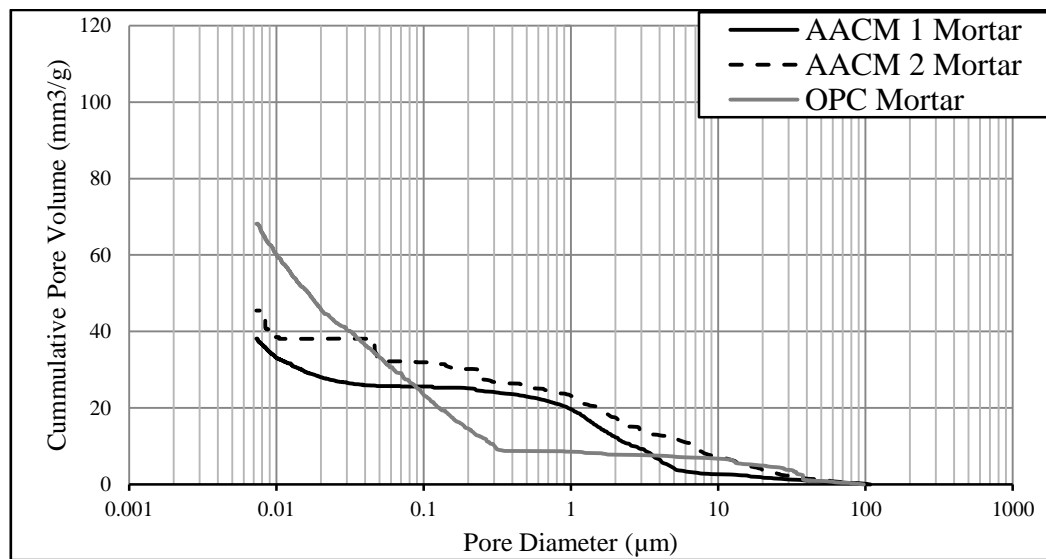The volume of intrudable pores (intrudable pore volume) within AACM 1, 2 and the control PC mortar matrix was determined under wet/dry, wet and dry curing from the cumulative

18

367   pore volume curves as shown in Figures 7, 8 and 9 respectively. Figure 10 shows the

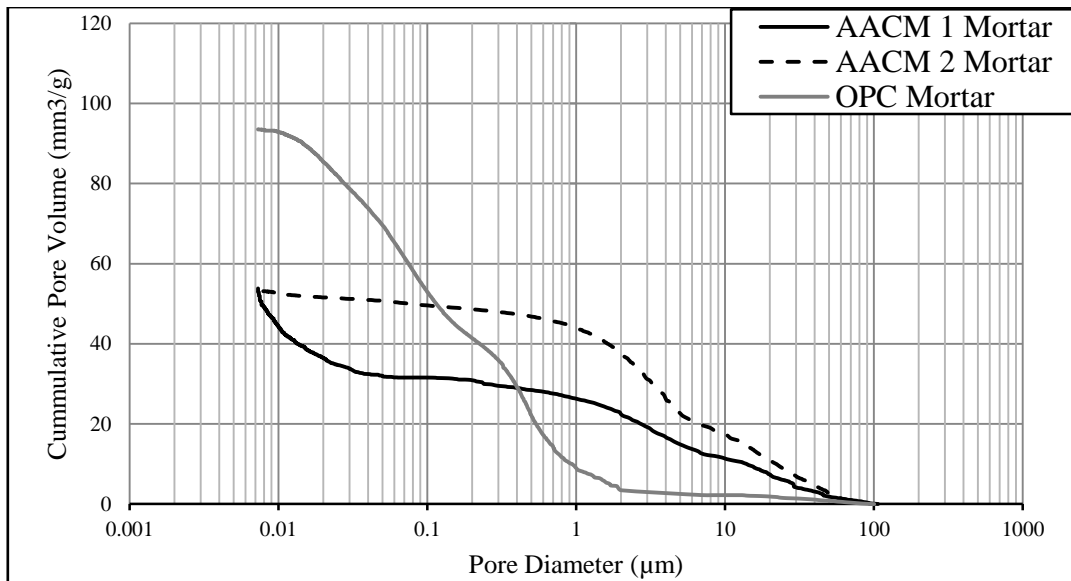368   intrudable pore volume.
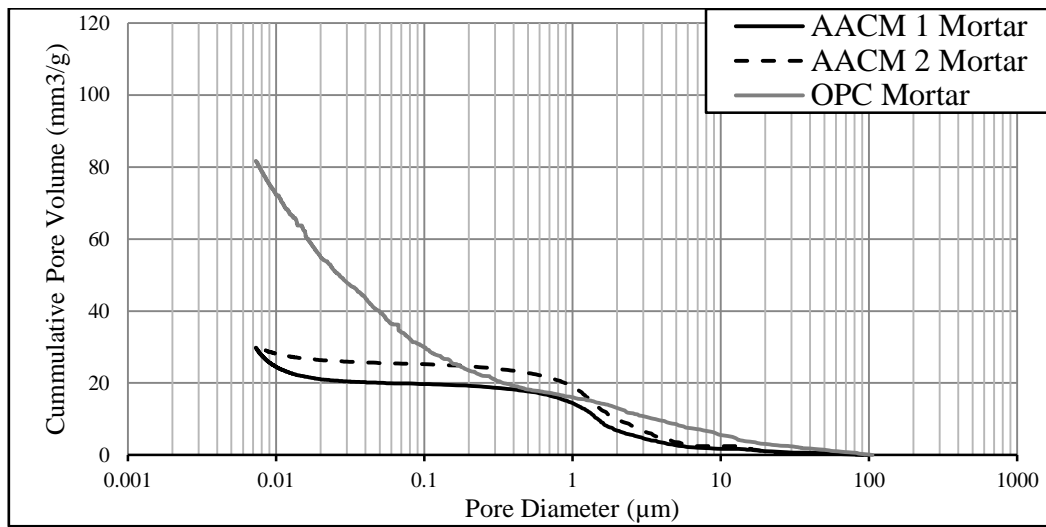
369

370   Fig. 7: Intrudable porosity for AACM 1, 2 and control OPC mortars under wet/dry curing
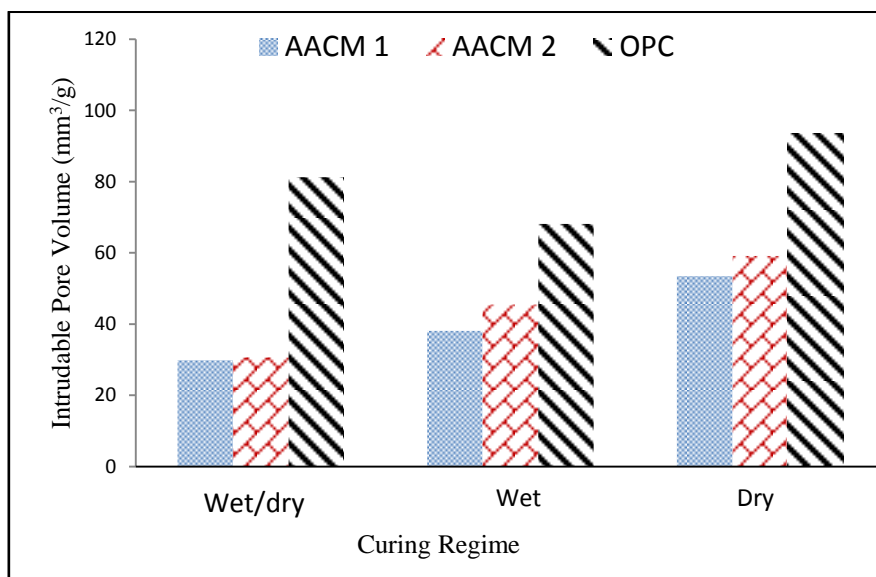

371

372   Fig. 8: Intrudable porosity for AACM 1, 2 and control OPC mortars under wet curing

373

374   Fig. 9: Intrudable porosity for AACM 1, 2 and control OPC mortars under dry curing

375

376   Fig.10: Intrudable pore volume for AACM 1, 2 and OPC mortars under wet/dry, wet and

377   dry curing

378   *Wet/dry curing*

379   AACM 1 and 2 mortars have lower intrudable pore volume of 29.68 mm^3/g and 30.17 mm^3/g

380   respectively compared with 81.62 mm^3/g for the control PC mortar as shown in Figures 7 and

381   10. The application of wet/dry curing to AACM concrete was observed to enhance its

382   resistance to chloride ingress under exposure to salt laden environment [15]. The initial 3

20

383 days wet curing followed by the 24 days dry curing in laboratory air under the wet/dry curing

384 method (Table 3) resulted in a lower intrudable pore volume in AACMs.

385 The intrudable pore volume for AACM 1 mortar is similar to the AACM 2 mortar (7.76%

386 activator dilution) at 29.68 mm^3/g and 30.17 mm^3/g respectively under wet/dry curing as

387 shown in Figures 7 and 10.

388 *Wet curing*

389 The wet curing of the control PC mortar resulted in an intrudable pore volume of 68.16

390 mm^3/g (Figures 8 and 10) compared with 81.62 mm^3/g and 93.51 mm^3/g for wet/dry and dry

391 curing respectively (Figures 7 and 9). The wet curing method usually provides the best

392 mechanical and durability properties for PC concrete due to saturation of its pore spaces with

393 water which aid cement hydration. *Powers* [31] and *Patel et al* [32] observed that the

394 hydration of PC concrete is greatly reduced when the relative humidity within the pore spaces

395 drops below 80%. Since both the wet/dry and dry curing methods exposed the control PC

396 mortar to laboratory air (R.H. 65%) before cement paste hydration was completed, it resulted

397 in more intrudable pores than under wet curing.

398 The intrudable pore volume of AACM 1 mortar (38.14 mm^3/g) under wet curing (Fig. 8) is

399 more than (29.68 mm^3/g) under wet/dry curing (Fig. 7). AACM 2 mortar also shows a

400 similarly higher intrudable pore volume under wet curing (Fig. 8).

401 *Dry Curing*

402 AACM 1 mortar has an intrudable porosity of 53.44 mm^3/g compared with 93.51 mm^3/g for

403 the control PC mortar under dry curing (Figures 9 and 10). The results presented in Figures 7,

404 8, 9 and 10 indicate that AACM 1 and 2 mortars possess significantly less intruded pore

405 volume than the control PC mortar under the three curing conditions.

406 *3.3.2   Critical and threshold pore diameters*

407   The critical and threshold pore diameters of a concrete matrix influence its durability

408   properties [29,30,33]. Lower values of these parameters represent enhanced durability

409   properties. AACM mortars under wet/dry curing had the lowest critical and threshold pore

410   diameters, followed by wet and dry curing. For example, AACM 1 had critical pore diameter

411   of 0.0073 μm both under wet/dry and wet curing and 0.0075 μm under dry curing (Table 4).

412   The corresponding threshold pore diameter was 0.013 μm, 0.014 μm and 0.025 μm. The

413   higher dilution of alkali activator in AACM 2 increased the critical and threshold pore

414   diameters as shown in Table 4. This pattern is similar for the three curing regimes wet/dry,

415   wet and dry. The difference in values under the three curing conditions is more pronounced

416   for the AACM 2 mix than AACM 1.

417   On the other hand, PC mortar under wet curing has the lowest critical and threshold pore

418   diameters compared with wet/dry and dry curing. The critical pore diamters are 0.016 μm,

419   0.049 μm and 1.07 μm under wet, wet/dry and dry curing respectively. The corresponding

420   threshold pore diameters are 0.28 μm, 0.35 μm and 1.12 μm in Table 4. The pore blocking

421   effect in PC concrete was proposed by *Khatib and Mangat* [34] for the wet curing regime.

422   The availability of water during curing allowed for more hydration to take place resulting in

423   the formation of more calcium silicate gel thereby reducing the critical and threshold pores.

424   AACM mortars displayed lower critical and threshold pore diameters than PC concrete.

425   Therefore, the durability properties of AACM mortars are expected to be superior to the PC

426   mortar. Early results from a comprehensive durability study by the authors indicate that

427   chloride diffusion in the PC mortar is greater than the AACM mixes [15]. The relationship

428   between chloride diffusion and the critical and threshold diameters will be addressed in a

429   future paper by the authors.

430   *3.3.3 Porosity of AACM and PC mortar*

431   The relationship between porosity and incremental pore diameter range of AACM 1 and the

432   control PC mortars under wet/dry, wet and dry curing are shown in Figures 11, 12 and 13

433   respectively.
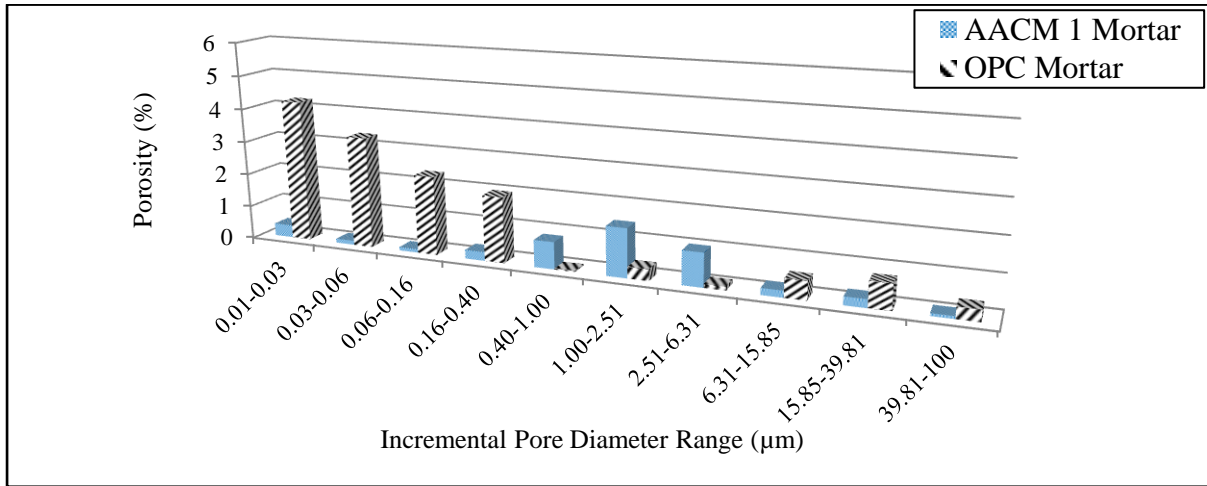
434

435   Figure 11: Relationship between porosity and incremental pore diameter (μm) range for AACM 1 and
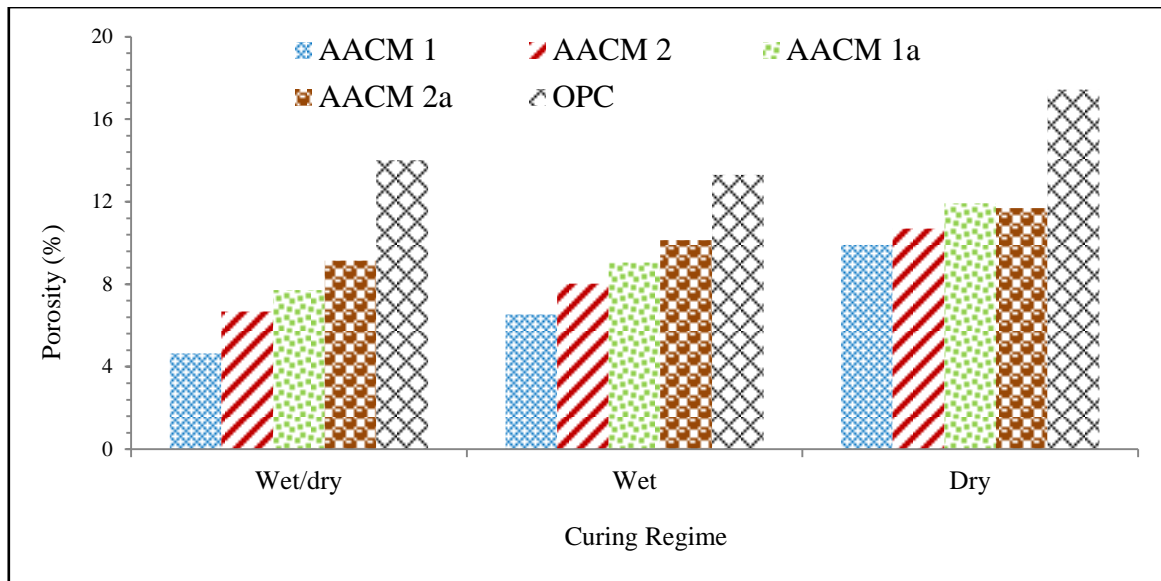
436   control OPC mortars under wet/dry curing.
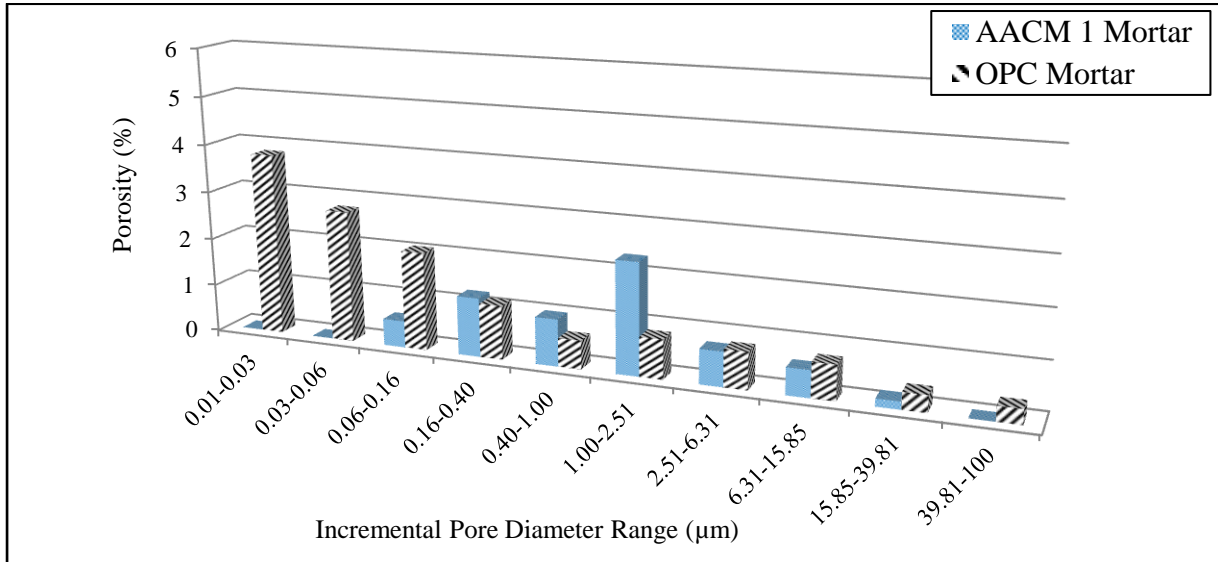
437

438   Figure 12: Relationship between porosity and incremental pore diameter (μm) range for AACM 1 and

439   control OPC mortars under wet curing.
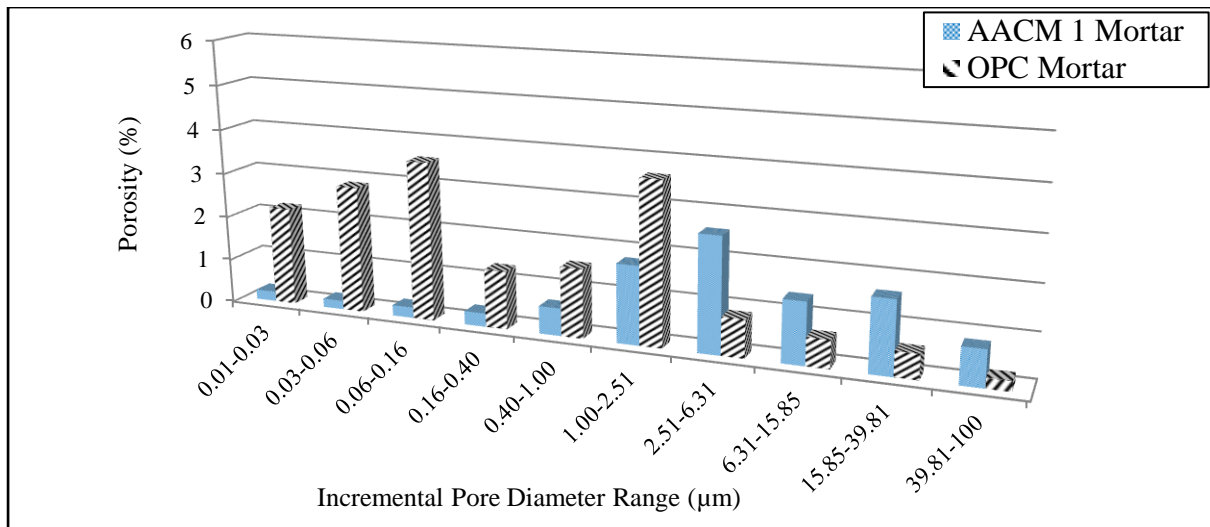
Figure 13: Relationship between porosity and incremental pore diameter (μm) range for AACM 1 and control OPC mortars under dry curing.

The figures show that the porosity of AACM 1 mortar is distributed along a limited range of pore diameters with more significant porosity at larger diameters. On the other hand, the control PC mortar has its porosity distributed along the whole range of pore diameters with more significant porosity at smaller diameters. The AACM mortars show a distinctively large volume of pores within the capillary pore zone (>0.16 μm) while PC mortars have a large volume of pores within the gel pore zone (<0.16 μm). For example, the percentage of capillary pore volume is 4.04% and 3.19% for AACM 1 and PC mortars respectively under wet/dry curing. The corresponding gel pore volume is 0.60% and 10.83%

451

452   Figure 14: Effective porosity of AACM and control OPC mortars under wet/dry, wet and dry
453   curing.

454   Fig. 14 shows the effective porosity of AACM 1 and the control PC mortars under wet/dry,

455   wet and dry curing. This is the summation of the incremental pore volumes in Figures 11, 12

456   and 13. The porosity of AACM 1 mortar is much lower than the control PC mortar despite

457   the presence of larger pores in AACM 1 mortar. The porosity of AACM 1 mortar is 4.64%,

458   6.53% and 9.90% compared with 14.02%, 13.30% and 17.43% for the control PC mortar

459   under wet/dry, wet and dry curing respectively. The porosity for the corresponding AACM 2

460   mortar is 6.67%, 8.02% and 10.70%.

461   The porosity of AACM mix 1a is 7.71%, 9.05% and 11.93% for wet/dry, wet and dry curing

462   respectively. Each value is significantly lower than the corresponding value for PC mortar.

463   AACM mix 1a did not incorporate any admixtures (SRA and R42) and, therefore, is directly

464   comparable with the PC mortar. The porosity of AACM mix 2a is similarly lower than the

465   PC mortar. The results confirm the lower porosity of the AACM mixes.

466   The wet/dry curing is optimum for AACM mortar while wet curing is best for the control PC

467   mortar, the latter being a well-established fact.

468   *RILEM TC 224* [2] reported that the total porosity (i.e. summation of both gel and capillary

469   pores) of AACM is somewhat similar or sometimes higher than comparative PC. The

470   contrary results of this study show that the total pore volume was higher in PC mortar than in

471   AACM mortar. Nevertheless, a higher capillary pore volume was observed in AACMs while

472   their gel pore volume was much lower than PC mortar. For example, AACM 1 and 2 mortar

473   has higher percentage of capillary pore volume of 4.04% and 5.69% respectively compared

474   with 3.19% for the control PC mortar under wet/dry curing (Table 4, Figures 11, 12 and 13).

475   On the other hand, the percentage of gel pore volume of 0.60% and 0.98% in AACM 1 and 2

476   respectively was much lower than 10.83% for PC mortar under wet/dry curing. A similar

477   trend is observed under wet and dry curing (Table 4, Figures 11, 12 and 13).

478   *3.3.4   Strength-porosity relationship of AACM mortars*

479   Strength and porosity data of AACM mixes 1, 2, 1a and 2a (Table 1) are considered in this

480   section together with the data for similar AACM mixes which were prepared with other

481   activator dilutions under 4%. The same mix proportions and test procedures outlined in the

482   paper were used for these mixes. The strength-porosity relationship of all the AACM mortars

483   under wet/dry, wet and dry curing together with the combined plot of wet/dry and dry curing

484   is shown in Figure 15. The best fit lines provide a non-linear plot according to the following

485   relationship proposed for porous materials by *Balshin* [35]

$$\sigma = \sigma_0(100\% - P)^n \qquad\qquad 2$$

486   Where σ = Compressive strength, σ_0 = Compressive strength of fully dense material at 0%

487   porosity, P = Porosity and n = Constant.

$$\Delta = 143.6\,(100\% - P)^{0.37}$$
$$R^2 = 0.71$$

$$\Delta = 136.7\,(100\% - P)^{0.42}$$
$$R^2 = 0.68$$
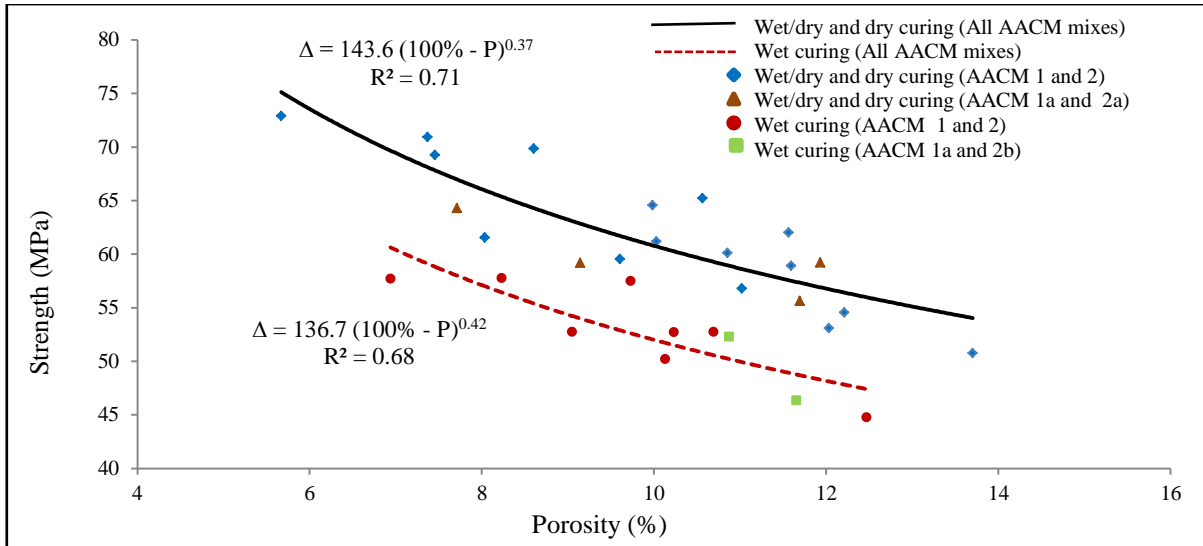
488

489   Figure 15: Strength- porosity relationship of AACM mortars under different curing.

490   A non-linear regression analysis of the data in Fig. 15 using equation 2 provided the

491   following best-fit equation for the combined wet/dry and dry cured AACM mixes.

$$6 = 143.6(100\% - P)^{0.37} \qquad\qquad 3$$

492   With a coefficient of correlation, $R^2 = 0.71$

493   The corresponding relationship for the wet cured AACM mortars is given by the following

494   equation:

$$6 = 136.7(100\% - P)^{0.42} \qquad\qquad 4$$

495   With a coefficient of correlation, $R^2 = 0.68$

496   AACM mortar subjected to wet/dry curing had the lowest porosity and highest strength. The

497   initial wet curing aided the production of more geopolymerisation while the subsequent dry

498   curing resulted in increased compressive strength [11]. AACM mortar subjected to wet/dry

499   and dry curing had a higher strength than wet curing in the same range of porosity as shown

500   in Fig. 15. For example from the best-fit relationships, the compressive strength at a porosity

27

501   of 10% is 61.2 MPa and 52.7 MPa under wet/dry and wet curing respectively. This indicates

502   an additional effect to porosity which enhances the strength of dry cured AACMs. This can

503   be due to enhanced strength of the geopolymerisation products with dry curing, including

504   increased bond within the geopolymer structure. The initial wet curing also favours the

505   hydration reactions of any high calcium compounds in the AACM binders. Therefore, the

506   optimum curing for strength-porosity relationship in AACMs is achieved under wet/dry

507   curing.

508   **4.0   Conclusions**

509   The paper presents an investigation on the effect of wet, wet/dry and dry curing on the pore

510   size distribution, porosity and strength of an alkali activated cementitious (AACM) mortar

511   and a comparative PC mortar. The AACM mixes were made with and without admixtures

512   (SRA and R42). The following conclusions can be drawn from the results of the study:

513   1) The wet/dry curing regime produces the highest compressive strength in AACM

514   mortars while it is wet curing for the control OPC mortar. For example, the 28 day

515   strength of AACM 1 mix under wet/dry, wet and dry curing was 70.9MPa,

516   57.9MPa and 61.2MPa respectively while it was 65.2 MPa, 46.4MPa and 54.6MPa

517   for AACM 2. The corresponding values of 43.4 MPa, 51.4 MPa and 42.3 MPa

518   were observed for OPC mortar.

519   2) AACM mortar develops a bimodal micropore distribution which is influenced by

520   the type of curing and the activator dilution. Wet/dry curing (3 days in water

521   followed by 24 days in air) provides an optimum pore structure for AACM. OPC

522   mortar develops a unimodal pore structure which is optimum under wet curing.

523   3) Higher activator concentration, within the range used, results in improved strength

524   and a more refined pore structure. For example, the strength of AACM mortar

525   under wet/dry curing with 0% activator dilution (AACM 1) is 70.9MPa compared

526   with 65.2MPa for AACM mortar with 7.76% activator dilution (AACM 2). Their

527   corresponding porosity is 4.64% and 6.67%.

528 4) Wet/dry curing of AACM mortar produces the lowest porosity and pore volume.

529   The porosity of AACM mixes is much lower than the control OPC mortar for each

530   curing condition. For example, AACM 1 mix under wet/dry, wet and dry curing

531   had a porosity of 4.64%, 6.53% and 9.90% respectively. In comparison, the control

532   OPC mortar under wet/dry, wet and dry curing had a porosity of 14.02%, 13.30%

533   and 17.43% respectively, giving the lowest porosity under wet curing.

534 5) The threshold pore diameters of AACM mixes, which influence durability

535   properties, are at least an order of magnitude lower than for the control OPC mixes.

536   For example, the threshold diameters for AACM 1 mortar under wet/dry, wet and

537   dry curing are 0.013 µm, 0.014 µm, and 0.025 µm respectively. The corresponding

538   values for the control OPC mortar are 0.35 µm, 0.28 µm, and 1.12 µm.

539 6) The volume of gel pores, within the range of 0.005 µm to 0.01 µm, in AACM

540   mortars is less than the control OPC mortar. On the other hand, the volume of

541   capillary pores, within the range of 0.01 µm to 100 µm pore diameter, is higher in

542   AACM mortars. However, the total porosity (summation of both gel and capillary

543   pores) is higher in the control OPC mortar than in AACM mortars. For example,

544   the gel porosity in AACM 1 and OPC mortar is 0.60% and 10.83% respectively

545   while their corresponding capillary porosity is 4.04% and 3.19% under wet/dry

546   curing.

547 7) The inclusion of a shrinkage reducing and retarding admixture in AACMs

548   enhances strength and produces a more refined pore structure particularly under

549   wet/dry and dry curing. AACM mortars, both with and without admixtures, have

29

550   superior strength and a more refined pore structure than the control OPC mortar

551   under wet/dry and dry curing.

    8) The strength-porosity relationship of AACM mortars under combined wet/dry

and dry curing is as follows: $6 = 143.6(100\% - P)^{0.37}$ with a coefficient of

correlation $R^2 = 0.71$. The relationship under wet curing is given by:

$6 = 136.7(100\% - P)^{0.42}$ with $R^2 = 0.68$. For any given porosity, the

strength is lower under wet curing.

552 Acknowledgments

559 References

560 [1]   P.C. Aïtcin, Cements of yesterday and today - concrete of tomorrow, Cem. Concr. Res. 30

561   (2000) 1349–1359. doi:10.1016/S0008-8846(00)00365-3.

562 [2]   John L. Provis, J.S.J. van Deventer, Alkali-Activated Materials State-of-the-Art Report,

563   RILEM TC 224-AAM, 2014.

564 [3]   N.A. Madlool, R. Saidur, M.S. Hossain, N.A. Rahim, A critical review on energy use and

565   savings in the cement industries, Renew. Sustain. Energy Rev. 15 (2011) 2042–2060.

566   doi:10.1016/j.rser.2011.01.005.

567 [4]   P. Mangat, P. Lambert, Sustainability of alkali-activated cementitious materials and

568   geopolymers, in: Sustain. Constr. Mater., Elsevier Ltd, 2016: pp. 459–476. doi:10.1016/B978-

569   0-08-100370-1.00018-4.

570 [5]   A.M. Neville, Properties of Concrete, Pearson Education Limited, 2011.

571 [6] R. Kumar, B. Bhattacharjee, Assessment of permeation quality of concrete through mercury

572 intrusion porosimetry, Cem. Concr. Res. 34 (2004) 321–328.

573 doi:10.1016/j.cemconres.2003.08.013.

574 [7] K.D. Stanish, R.D. Hooton, M.D.A. Thomas, Testing the Chloride Penetration Resistance of

575 Concrete: A Literature Review, 1997.

576 [8] J.A. Larbi, Microstructure of the interfacial zone around aggregate particles in concrete,

577 Heron. 39 (1993) 1–69.

578 [9] D. Mindess, Sidney; Young, J. Francis; Darwin, Concrete, Prentice Hall, Pearson Education,

579 Inc. Upper Saddle River, NJ 07458, U.S.A., 2003.

580 [10] Y. Li, J. Li, Capillary tension theory for prediction of early autogenous shrinkage of self-

581 consolidating concrete, Constr. Build. Mater. 53 (2014) 511–516.

582 doi:10.1016/j.conbuildmat.2013.12.010.

583 [11] J.C. Petermann, A. Saeed, M.I. Hammons, Alkali-activated geopolymers: a literature review

584 air force research laboratory materials and manufacturing directorate, 2010.

585 [12] T. Medina-Serna, S. Arredondo-Rea, J. Gómez-Soberón, C. Rosas-Casarez, R. Corral-Higuera,

586 Effect of curing temperature in the alkali-activated blast-furnace slag paste and their structural

587 influence of porosity, Adv. Sci. Technol. Res. J. 10 (2016) 74–79.

588 doi:10.12913/22998624/64021.

589 [13] G. Fang, W.K. Ho, W. Tu, M. Zhang, Workability and mechanical properties of alkali-

590 activated fly ash-slag concrete cured at ambient temperature, Constr. Build. Mater. 172 (2018)

591 476–487. doi:10.1016/j.conbuildmat.2018.04.008.

592 [14] A. Cwirzen, R. Engblom, J. Punkki, K. Habermehl-Cwirzen, Effects of curing: comparison of

593 optimised alkali-activated PC-FA-BFS and PC concretes, Mag. Concr. Res. 66 (2014) 315–

594 323. doi:10.1680/macr.13.00231.

595 [15] Olalekan.O. Ojedokun and Pal. S. Mangat, Chloride Diffusion in Alkali Activated Concrete,

596 in: II Int. Conf. Concr. Sustain., 2016: pp. 521–531.

597 [16] BS ISO 15901-1:2016 - Evaluation of pore size distribution and porosity of solid materials by

598 mercury porosimetry and gas adsorption. Mercury porosimetry, 2016.

599   [17]   BS EN196-1, Methods of testing cement - Part 1: Determination of strength, Eur. Stand.

600   (2005) 1–33. doi:10.1111/j.1748-720X.1990.tb01123.x.

601   [18]   BS EN 12350-5 Testing fresh concrete - Part 5: Flow Table Test, Eur. Stand. (2009).

602   doi:10.1007/s13398-014-0173-7.2.

603   [19]   H. Jansson, D. Bernin, K. Ramser, Silicate species of water glass and insights for alkali-

604   activated green cement, AIP Adv. 5 (2015) 67167. doi:10.1063/1.4923371.

605   [20]   V. Sathish Kumar, N. Ganesan, P. V Indira, Effect of Molarity of Sodium Hydroxide and

606   Curing Method on the Compressive Strength of Ternary Blend Geopolymer Concrete, IOP

607   Conf. Ser. Earth Environ. Sci. 80 (2017) 12011. doi:10.1088/1755-1315/80/1/012011.

608   [21]   BS EN 12390-3:2009 Testing Hardened Concrete Part 3: Compressive Strength of Test

609   Specimens, 2009.

610   [22]   BS EN 12390-7:2009, Testing hardened concrete. Density of hardened concrete – BSI British

611   Standards, in: n.d. https://shop.bsigroup.com/ProductDetail/?pid=000000000030164912

612   (accessed June 21, 2018).

613   [23]   N. Hearn, R.D. Hooton, Sample mass and dimension effects on mercury intrusion porosimetry

614   results, Cem. Concr. Res. 22 (1992) 970–980. doi:10.1016/0008-8846(92)90121-B.

615   [24]   M.M. Reda Taha, A.S. El-Dieb, N.G. Shrive, Sorptivity: a reliable measurement for surface

616   absorption of masonry brick units, Mater. Struct. Constr. 34 (2001) 438–445.

617   [25]   M.I. Mousa, M.G. Mahdy, A.H. Abdel-Reheem, A.Z. Yehia, Self-curing concrete types; water

618   retention and durability, Alexandria Eng. J. 54 (2015) 565–575.

619   doi:10.1016/J.AEJ.2015.03.027.

620   [26]   K. Tan, O.E. Gjorv, Performance of concrete under different curing conditions, Cem. Concr.

621   Res. 26 (1996) 355–361.

622   [27]   D. Khale, R. Chaudhary, Mechanism of geopolymerization and factors influencing its

623   development: A review, J. Mater. Sci. 42 (2007) 729–746. doi:10.1007/s10853-006-0401-4.

624   [28]   A.C. Garrabrants, F. Sanchez, D.S. Kosson, Leaching model for a cement mortar exposed to

625   intermittent wetting and drying, AIChE J. 49 (2003) 1317–1333. doi:10.1002/aic.690490523.

626   [29]   K.K. ALIGIZAKI, Pore structure of cement-based materials: testing, interpretation and

627   requirements, Taylor & Francis, Abingdon [England], 2006.

628   [30]   H. Ma, Mercury intrusion porosimetry in concrete technology: Tips in measurement, pore

629   structure parameter acquisition and application, J. Porous Mater. 21 (2014) 207–215.

630   doi:10.1007/s10934-013-9765-4.

631   [31]   T.C. Powers, A discussion of cement hydration in relation to the curing of concrete, Highw.

632   Res. Board Proc. 27 (1948). https://trid.trb.org/view.aspx?id=102345 (accessed June 29,

633   2017).

634   [32]   R.G. Patel, D.C. Killoh, L.J. Parrott, W.A. Gutteridge, Influence of curing at different relative

635   humidities upon compound reactions and porosity in Portland cement paste, Mater. Struct. 21

636   (1988) 192–197. doi:10.1007/bf02473055.

637   [33]   A.T.C. Guimarães, G. De Vera, F.T. Rodrigues, C. Antõn, M.A. Climent, Comparison

638   between Dcrit Considering the Abrupt Variation and Inflexion in the Concrete Mercury

639   Intrusion Porosimetry Curve, Exp. Tech. (2015). doi:10.1111/ext.12002.

640   [34]   J.M. Khatib, P.S. Mangat, Porosity of cement paste cured at 45C as a function of location

641   relative to casting position, Cem. Concr. Compos. 25 (2003) 97–108. doi:10.1016/S0958-

642   9465(01)00093-2.

643   [35]   Balshin M.Y., Relation of Mechanical Properties of Powder Metals and their Porosity and the

644   Ultimate Properties of Porous-Metal Ceramic Materials, 67 (1949) 831–834.